Available online at www.sciencedirect.com
SCIENCE DIRECT®
International Journal of Heat and Mass Transfer 48 (2005) 4973–4984
International Journal of HEAT and MASS TRANSFER
www.elsevier.com/locate/ijhmt

Effect of tube diameter on boiling heat transfer of R-134a in horizontal small-diameter tubes

Shizuo Saitoh [a,*], Hirofumi Daiguji [b], Eiji Hihara [b]

[a] Department of Mechanical Engineering, The University of Tokyo, 7-3-1 Hongo, Bunkyo-ku, Tokyo 113-8656, Japan
[b] Institute of Environmental Studies, Graduate School of Frontier Sciences, The University of Tokyo, 7-3-1 Hongo, Bunkyo-ku, Tokyo 113-8656, Japan

Received 3 September 2004
Available online 9 August 2005

Abstract

The boiling heat transfer of refrigerant R-134a flow in horizontal small-diameter tubes with inner diameter of 0.51, 1.12, and 3.1 mm was experimentally investigated. Local heat transfer coefficient and pressure drop were measured for a heat flux ranging from 5 to 39 kW/m^2, mass flux from 150 to 450 kg/m^2 s, evaporating temperature from 278.15 to 288.15 K, and inlet vapor quality from 0 to 0.2. Flow patterns were observed by using a high-speed video camera through a sight glass at the entrance of an evaporator. Results showed that with decreasing tube diameter, the local heat transfer coefficient starts decreasing at lower vapor quality. Although the effect of mass flux on the local heat transfer coefficient decreased with decreasing tube diameter, the effect of heat flux was strong in all three tubes. The measured pressure drop for the 3.1-mm-ID tube agreed well with that predicted by the Lockhart–Martinelli correlation, but when the inner tube diameter was 0.51 mm, the measured pressure drop agreed well with that predicted by the homogenous pressure drop model. With decreasing tube diameter, the flow inside a tube approached homogeneous flow. The contribution of forced convective evaporation to the boiling heat transfer decreases with decreasing the inner tube diameter.

1. Introduction

High efficiency, compact heat exchangers have recently received much attention in their use in air conditioning systems due to possible energy conservation. Fundamental data on boiling heat transfer, such as heat transfer coefficient and pressure drop, is essential for design and operation of heat exchangers. Despite extensive experimental data on flow boiling heat transfer in small-diameter tubes, the general characteristics have not yet been clarified. Table 1 summarizes recent experimental studies classified into single and multi path types, depending upon the flow path of the working fluid. Although studies on multi path flow yield more information for practical applications, clarifying the general characteristics of boiling flow in a small-diameter tube is difficult. Therefore, multi path flow studies are beyond the scope of this current study.

Based on reported local heat transfer coefficients, the regions of fluid flow and heat transfer in tubes with boiling flow can be classified as follows: (i) the region in

* Corresponding author. Tel.: +81 3 5841 6325; fax: +81 3 5841 6349.
E-mail address: saitoh@hee.k.u-tokyo.ac.jp (S. Saitoh).

0017-9310/$ - see front matter © 2005 Elsevier Ltd. All rights reserved.
doi:10.1016/j.ijheatmasstransfer.2005.03.035

Nomenclature

C_g	friction factor for gas, $C_g = 0.046$
C_l	friction factor for liquid, $C_l = 16$
c_{pl}	specific heat at constant pressure in liquid phase, J/kg K
D	inner diameter of a tube, m
f_{TP}	two-phase friction factor
G	mass flux, kg/m^2 s
g	acceleration of gravity, m/s^2
h_{exp}	experimental boiling heat transfer coefficient, W/m^2 K
h_l	liquid phase heat transfer coefficient, W/m^2 K $Re_l > 1000$, $h_l = 0.023\frac{\lambda_l}{D}(\frac{G_l D}{\mu_l})^{0.8}\times(\frac{c_{pl}\mu_l}{\lambda_l})^{1/3}$; $Re_l < 1000$, $h_l = \frac{4.36\lambda_l}{D}$
p	pressure, Pa
q	heat flux, W/m^2
Re	Reynolds number $Re_l = \frac{G_l D}{\mu_l}$, $Re_g = \frac{G_g D}{\mu_g}$
T_{evap}	evaporating temperature, K
T_{wall}	inside-wall temperature, K
T_{sat}	saturation temperature, K
U_g	superficial gas velocity, m/s
U_l	superficial liquid velocity, m/s
We	Weber number
x	vapor quality
X	Lockhart–Martinelli parameter $Re_l > 1000$, $Re_g > 1000$; $X = (\frac{1-x}{x})^{0.9}(\frac{\rho_g}{\rho_l})^{0.5}(\frac{\mu_l}{\mu_g})^{0.1}$; $Re_l < 1000$, $Re_g > 1000$; $X = (\frac{C_l}{C_g})^{0.5}Re_g^{-0.4}(\frac{G_l}{G_g})^{0.5}\times(\frac{\rho_g}{\rho_l})^{0.5}(\frac{\mu_l}{\mu_g})^{0.5}$
z	coordinate along the tube direction, m

Greek symbols

ζ	parameter in Baker's flow pattern map $\zeta = [(\frac{\rho_g}{\rho_a})(\frac{\rho_l}{\rho_w})]^{0.5}$
φ	parameter in Baker's flow pattern map $\varphi = \frac{\sigma_w}{\sigma_l}[\frac{\mu_l}{\mu_w}(\frac{\rho_w}{\rho_l})^2]^{1/3}$
λ	thermal conductivity, W/m K
μ	viscosity, Pa s
ρ	density, kg/m^3
σ	surface tension, N/m
ϕ	two-phase flow multiplier

Subscripts

a	air
g	gas-phase, vapor-phase
h	homogeneous
in	inlet
l	liquid-phase
TP	two-phase
w	water

which nucleate boiling is dominant, where the local heat transfer coefficient is affected mainly by the heat flux; (ii) the region in which convective evaporation is dominant, where the local heat transfer coefficient is affected mainly by the mass flux and vapor quality and (iii) the intermediate region, where neither nucleate boiling nor convective evaporation is dominant. Lin et al. [1,2] experimentally studied boiling flow of refrigerant R-141b in vertical pipes (1–3.6 mm in diameter) and in one square tube (2 mm × 2 mm), and reported that nucleate boiling was dominant at low vapor quality, and that convective boiling was dominant at high vapor quality. Lazarek and Black [3] experimentally studied boiling flow of refrigerant R-113 in a 3.15-mm-ID pipe, Bao et al. [4] studied boiling flow of refrigerants R-11 and R-123 in a 1.95-mm-ID channel, and Yu et al. [5] studied boiling flow of water in a small horizontal tube (2.98-mm-ID), and they all concluded that nucleate boiling was dominant. Tran et al. [6] experimentally studied flow boiling in a 2.46-mm-ID tube and in a rectangular channel (1.7 mm × 4.06 mm), and reported that nucleate boiling was dominant, and that the heat transfer characteristics did not depend on the channel geometry. Based on experiments using a 2.92-mm-ID horizontal tube, Wambsganss et al. [7] reported that the heat transfer coefficient strongly depended on heat flux, and weakly depended on mass flux and vapor quality. In contrast, Qu and Mudawar [8] reported that the dominant heat transfer mechanism for saturated flow boiling in microchannels was forced convective boiling and not nucleate boiling, because the heat transfer coefficient for flow boiling strongly depended on mass flux and weakly depended on heat flux. Sumith et al. [9] experimentally studied the heat transfer of boiling water flow in a 1.45-mm-ID vertical tube, and reported that the heat transfer was dominated by forced convection when the heat flux was higher than 200 kW/m^2. Lee and Lee [10] studied flow boiling of refrigerant R-113 in three different rectangular channels (20 mm × 0.4 mm, 20 mm × 1.0 mm, and 20 mm × 2.0 mm), and reported that the heat transfer coefficient increased with increasing mass flux and vapor quality, whereas the effect of heat flux was insignificant.

Table 1
Studies on the heat transfer characteristics in small-diameter tubes

References	Working fluid	Tube geometry; diameter or size (mm) (length (mm)); material; orientation	Pressure (MPa)	Heat flux (kW/m^2)	Mass flux ($kg/m^2\,s$)	Vapor quality
Lin et al. [1]	R-141b	Circular; ID = 1.0 ($l = 500$); –; vertical	0.135–0.22	10–1150	300–2000	−0.2 to 0.99
Lin et al. [2]	R-141b	Circular/rectangular; ID = 1.1 ($l = 500$), 1.8 ($l = 496$), 2.8 ($l = 498$), 3.6 ($l = 454$)/2 × 2 ($l = 454$); –; vertical	0.1–0.3	1–300	50–3500	0–1.0
Lazarek and Black [3]	R-113	Circular; ID = 3.15 ($l = 123$, 246); stainless; vertical	0.13–0.41	14–380	125–750	−0.2 to 0.6
Bao et al. [4]	R-11, R-123	Circular; ID = 1.95 ($l = 270$); copper; horizontal	0.2–0.5	5–200	50–1800	−0.3 to 0.9
Yu et al. [5]	Water	Circular; ID = 2.98 ($l = 910$); stainless; horizontal	0.2	50–300	50–200	0–1.0
Tran et al. [6]	R-12, R-113	Circular/rectangular; ID = 2.46 ($l = 870$)/1.7 × 4.06 ($l = 870$); brass; horizontal	0.51, 0.82	3.6–129	44–832	−0.94
Wambsganss et al. [7]	R-113	Circular; ID = 2.92 ($l = 368$); stainless; horizontal	0.124–0.16	8.8–90.75	50–300	0–0.9
Qu and Mudawar [8]	Water	Rectangular; 0.231 × 0.713 ($l = 44.8$), parallel 21; copper; horizontal	0.117	220–1300	135–402	−0.2
Sumith et al. [9]	Water	Circular; ID = 1.45 ($l = 100$); stainless; vertical	0.1	10–715	23.4–152.7	0–0.8
Lee and Lee [10]	R-113	Rectangular; 20 × 0.4, 20 × 1, 20 × 2 ($l = 300$); stainless; horizontal	–	3–15	50–200	0.15–0.75
Yan and Lin [11]	R-134a	Circular; ID = 2 ($l = 200$), parallel 28; –; horizontal	0.35–0.8	5–20	50–200	0.1–0.9
Oh et al. [12]	R-134a	Circular; ID = 0.75, 1, 2 ($l = 500$); copper; horizontal	0.4	10, 15, 20	240–720	0.1–1.0
Kuwahara et al. [13]	R-134a	Circular; ID = 0.84, 2 ($l = 880$); stainless; horizontal	0.92	1.16–46.8	100–600	0.01–0.84
Kew and Cornwell [14]	R-141b	Circular; ID = 1.39–3.69 ($l = 500$); stainless; horizontal	–	9.7–90	188–1480	−0.05 to 0.9
Pettersen [26]	CO_2	Circular; ID = 0.81 ($l = 540$), parallel 25; aluminum; horizontal	3.5–6.4	5–20	190–570	0.2–0.8

Several studies have compared the boiling heat transfer and pressure drop in different diameter tubes. Yan and Lin [11] experimentally investigated evaporation heat transfer and pressure drop for R-134a flowing in a 2.0-mm-ID tube, and found that the evaporation heat transfer coefficient in the 2.0-mm-ID tube was about 30–80% higher than that in the 8.0-mm-ID tube. Oh et al. [12] experimentally studied the evaporation heat transfer for R-134a flowing in three different copper tubes (0.75-, 1.0-, and 2.0-mm-ID), and reported that the heat transfer coefficient of the 1.0-mm-ID tube was higher than that of the 2.0-mm-ID tube when the vapor quality was less than 0.6, and that the dryout point moved to lower vapor quality with decreasing tube diameter. Kuwahara et al. [13] experimentally investigated the heat transfer characteristics and flow patterns for evaporation of R-134a in two different tubes (0.84- and 2.0-mm-ID), and reported that the characteristics of evaporation heat transfer for the small tube were similar to those for the large tube.

To clarify the characteristics of flow boiling heat transfer in small tubes, the relation between the heat transfer and two-phase flow patterns has been studied. For example, Based on experiments of flow boiling with R-141b in different diameter tubes (1.39- to 3.69-mm-ID), Kew and Cornwell [14] reported that two-phase flow in small tubes (<3.69-mm-ID) slightly differed from those in large tubes, and classified the flow types into the following three types: isolated bubble flow, confined bubble flow, and annular-slug flow. They also reported that intermittent dryout occurred at very low vapor quality. Based on experiments of air–water two-phase horizontal flow in 1.1- and 1.45-mm-ID tubes, Triplett et al. [15] classified the two-phase flow into five types: bubbly flow, slug flow, churn flow, slug–annular flow and annular flow. Kawahara et al. [16] classified two-phase flow into two types, namely, intermittent flow and semi-annular flow, and classified further these two flows into five types depending on the gas–liquid interfacial configuration. Based on experiments of air–water and R-134a two-phase flow in 1-, 2- and 3-mm-ID tubes, Yang and Shieh [17] concluded that surface tension is an important factor in determining the flow patterns in small tubes.

In the flow boiling heat transfer in small tubes (<3-mm-ID), the general characteristics and the effects of tube diameter and flow pattern on such heat transfer have not yet been clarified [18]. In the present study, the effect of tube diameter on the boiling heat transfer was systematically investigated to provide useful data for the design of compact heat exchangers using small tubes. The effect was studied by measuring the heat transfer coefficient and pressure drop and observing the flow patterns of the refrigerant R-134a in three different horizontal smooth tubes (0.51-, 1.12- and 3.1-mm-ID) for a range of heat flux (q), mass flux (G), inlet vapor quality (x_{in}), and evaporating temperature (T_{evap}).

2. Experimental apparatus and procedure

Fig. 1 shows a schematic of the experimental system used to measure the heat transfer coefficient and pressure drop and observing the flow patterns of the refrigerant R-134a. The system consisted of two loops, a 'test loop' and 'main loop', to provide well-controlled flow of refrigerant to the test tube. The test loop contained a Coriolis-type flowmeter, a refrigerant temperature controller, a manual expansion valve, a test tube (evaporator), and two sight glasses. The working fluid was refrigerant R-134a with a purity of 99.9%. To reduce the heat transfer between the test tube and its surroundings, the entire test tube was placed inside a duct in which the air at the evaporating temperature was circulated. The flow rate and inlet pressure of R-134a were set by controlling the frequency of the compressor and the opening of the expansion valve. The vapor quality at the inlet of the test tube (x_{in}) was set by changing the temperature of the refrigerant.

Table 2 lists the dimensions of the three test tubes. The length of each tube was determined such that the difference in vapor quality between the inlet and outlet of the test tube was $\Delta x = 0.9$ when the mass flow rate of the refrigerant (i.e., mass flux G) was 300 kg/m^2 s and the heat flux q was 12 kW/m^2. Fig. 2a shows details of the measuring points of temperature and pressure with the 3.1-mm-ID test tube. Each test tube was heated by direct electrification via an electrode by using a DC power supply connected to electrode soldered at both ends and at the center of the test tube as shown in

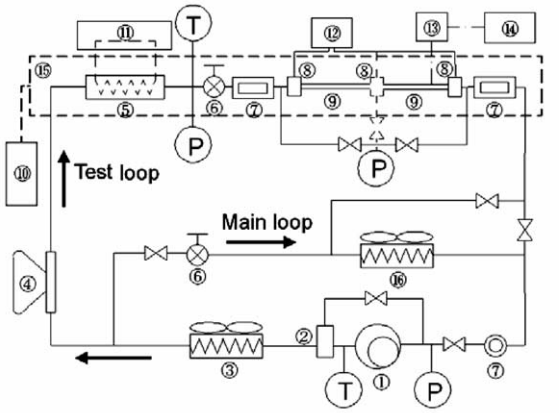

Fig. 1. Schematic of experimental system used to measure flow boiling heat transfer and pressure drop.

Table 2
Dimensions of small-diameter tubes

Material: SUS304		
ID (mm)	Wall thickness (mm)	Length (mm)
0.51	0.15	550
1.12	0.18	935
3.1	0.1	3235

Fig. 2a. The heated length (L_{heat}) of the tube was determined such that the difference in vapor quality between the inlet and outlet of the test tube was $\Delta x = 0.9$ depending on the mass flux and heat flux. For the 3.1-mm-ID tube, $L_{heat} = 3.24$ m at $G = 300$ kg/m^2 s and $q = 12$ kW/m^2, and $L_{heat} = 1.62$ m at $G = 300$ kg/m^2 s and $q = 24$ kW/m^2. At the inlet and outlet of the tube, the temperature of the refrigerant was measured by using 1-mm-OD T-type sheathed thermocouples and the pressure by using a precision aneroid manometer. Fig. 2b shows details of the thermocouple installation on a test tube. Temperature of the outer surface of the test tube was measured midway between the top and bottom of the tube along the surface by using a 0.1-mm-OD T-type thermocouple and temperature of the inner wall of the tube was calculated from the measured temperature of the outer wall of the tube by using the Fourier's law. For electrical insulation, an 8-μm-thick Teflon sheet was inserted between each thermocouple and the test tube. Thermal contact between each thermocouple and the tube was improved by filling the gap with enamel paint.

A system of temperature measurement was calibrated by using a platinum resistance thermometer sensor (Chino, Model CNA) with an accuracy of ±0.03 K and a constant-temperature water bath (Tokyo-Rikakikai, Model NCB-2200) within a temperature fluctuation of ±0.05 K. The accuracy of the calibrated thermocouples was within ±0.1 K. The mass flow rate (and thus the mass flux, G) was measured by using a Coriolis-type flowmeter (Oval, Model E010S-IN-200) with an accuracy of ±0.1%. The pressure was measured by using a precision aneroid manometer (Nagano Keiki, Model NKS) with an accuracy of ±1.5 kPa. The electrical input power was measured by using a voltmeter and an ammeter, confirming that the heat generated by direct electrification was well transferred to the fluid and that the heat gain from surroundings was within 3%. The concentration of lubricant oil was measured by sampling the working fluid. The measured concentration was less than 0.1 wt.%, confirming that the effect of the oil on the boiling heat transfer and pressure drop was insignificant.

For a range of G, x, q, and T_{evap} as summarized in Table 3, the local heat transfer coefficient h_{exp} in the

Table 3
Experimental conditions

Refrigerant: R-134a			
Evaporating temperature (K): 278.15, 283.15, 288.15			
ID (mm)	Heat flux (kW/m^2)	Mass flux (kg/m^2 s)	Vapor quality
0.51	12–39	150–450	0.23–1.0
1.12	10–30	150–400	0.2–1.0
3.1	5–29	150–450	0.2–1.0

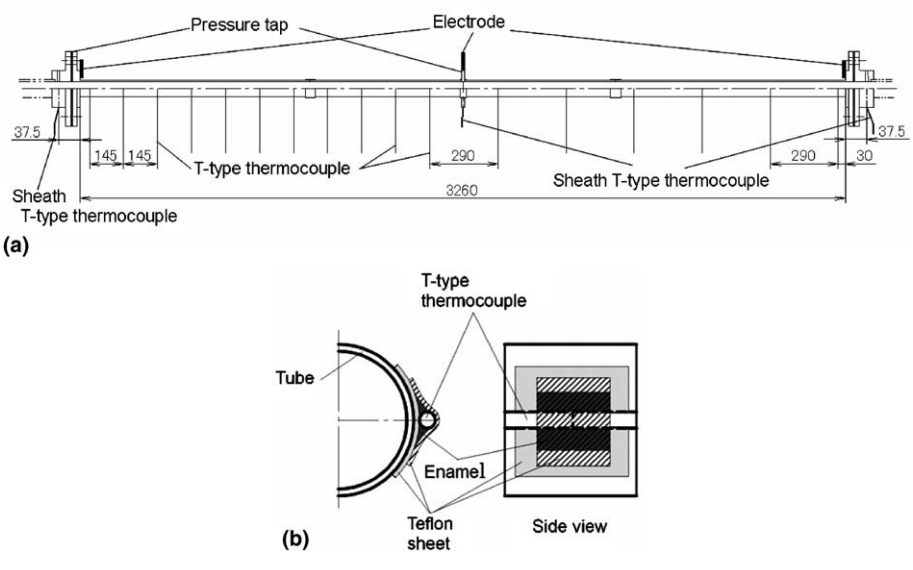

Fig. 2. Schematic of 3.1-mm-ID test tube: (a) entire test tube and (b) installation of thermocouple.

three tubes was determined using the following equation:

$$h_{\text{exp}} = \frac{q}{T_{\text{wall}} - T_{\text{sat}}} \tag{1}$$

where T_{wall} is the temperature at an inner wall, and T_{sat} is the saturation temperature at a local refrigerant pressure calculated by interpolation between the inlet and outlet pressures. Flow patterns were observed by using a high-speed video camera through a sight glass at the entrance of an evaporator. All experimental data were collected after steady state of temperature, pressure and refrigerant flow was achieved.

3. Results and discussion

3.1. Effect of mass flux (G) and heat flux (q) on boiling heat transfer

Fig. 3a–c show the effect of q and G on the boiling heat transfer for the three different diameter tubes. For

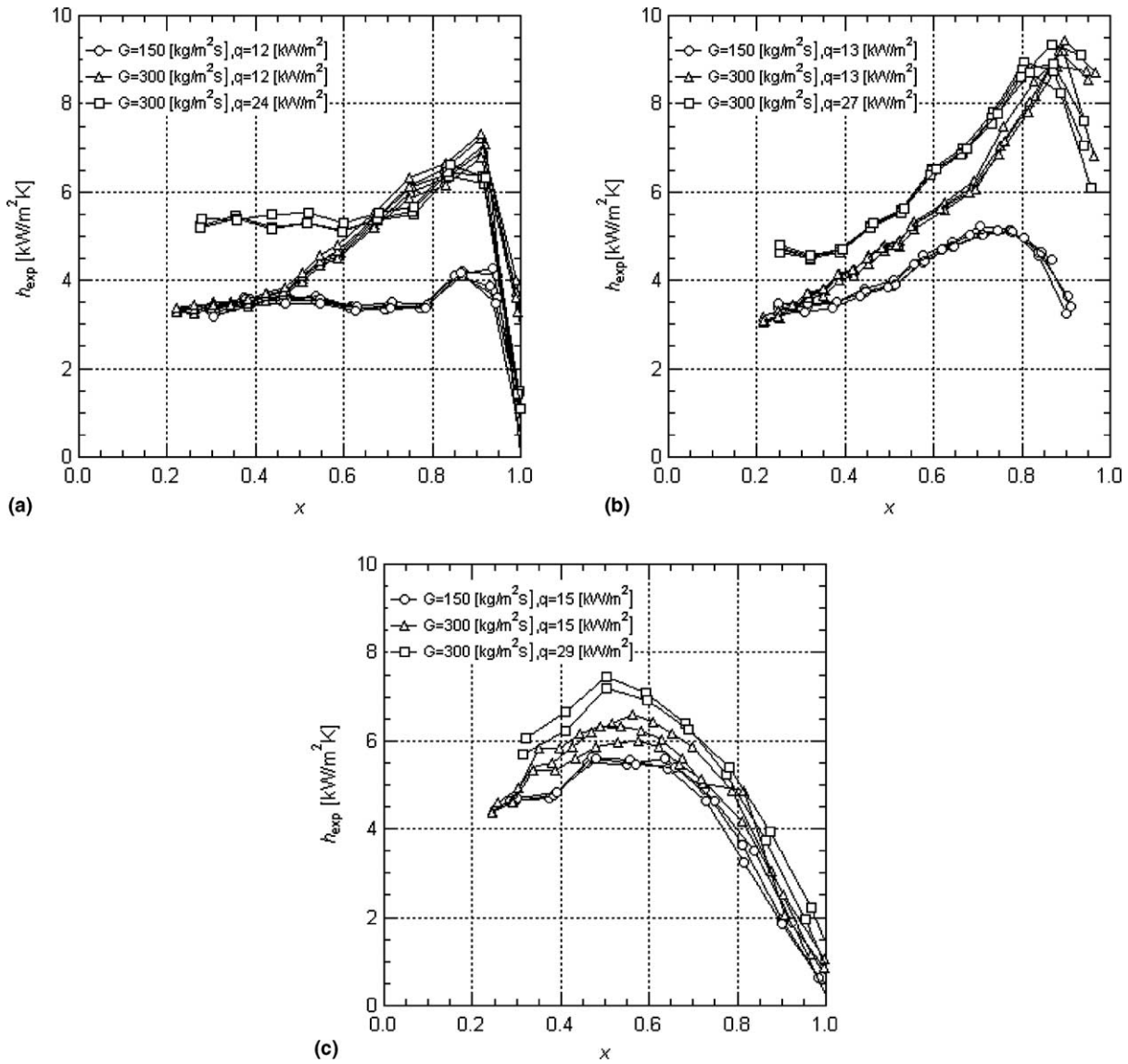

Fig. 3. Effect of heat flux (q) and mass flux (G) on heat transfer coefficient (h_{exp}) for three different diameter tubes: (a) 3.1-mm-ID; (b) 1.12-mm-ID and (c) 0.51-mm-ID.

the 3.1-mm-ID tube (Fig. 3a), in the low x region (<0.6), when G was fixed at 300 kg/m^2 s, h_{exp} for $q = 24$ kW/m^2 was higher than that for $q = 12$ kW/m^2, whereas when q was fixed at 12 kW/m^2, h_{exp} for $G = 150$ kg/m^2 s was similar to that for $G = 300$ kg/m^2 s. In contrast, in the high x region (>0.5), when q was fixed at 12 kW/m^2, h_{exp} for $G = 300$ kg/m^2 s was higher than that for $G = 150$ kg/m^2 s, whereas when G was fixed at 300 kg/m^2 s, h_{exp} for $q = 12$ kW/m^2 was similar to that for $q = 24$ kW/m^2. These experimental results suggest that in the low x region, nucleated boiling heat transfer was dominant, and in the high x region, forced convective evaporation was dominant. For the 1.12-mm-ID tube (Fig. 3b), h_{exp} was slightly higher than that for the 3.1-mm-ID tube (Fig. 3a), and the effects of q and G on h_{exp} were similar for both tubes. For the 0.51-mm-ID tube (Fig. 3c), h_{exp} increased with increasing q, but was not significantly affected by G. Among the three tubes, h_{exp} for the 0.51-mm-ID tube was the highest, when $x < 0.5$. As the ID is decreased, h_{exp} starts to decrease at lower x. The x at which h_{exp} started to decrease was 0.9 for the 3.1-mm-ID tube, between 0.8 and 0.9 for the 1.12-mm-ID tube, and between 0.5 and 0.6 for the 0.51-mm-ID tube.

3.2. Effect of flow pattern and inlet vapor quality (x_{in}) on boiling heat transfer

The flow patterns in small tubes and large tubes differ because the ratio of surface force to body force depends on the tube diameter. Flow patterns observed here were annular flow and intermittent flows, and the intermittent flows were classified further into plug flow and slug flow. Bubbly flow and stratified flow were not observed. Superficial gas velocity ranged from 0.023 to 15.04 m/s and superficial liquid velocity ranged from 0.011 to 0.318 m/s. For the 0.51-mm-ID tube, flow patterns were slug flow at low x and annular flow at high x. In the slug flow, bubbles elongated in the flow direction occupied a tube, and a smooth liquid film was formed along the tube wall. The size of the bubbles increased downstream, and the transition from slug flow to annular flow occurred in the middle of the tube. For 1.12- and 3.1-mm-ID tubes, bubbles were evident at the upper part of tubes, and the surface roughness of the bubbles increased downstream. Ghiaasiaan and Abdel-Khalik [19] reported that three dimensionless parameters govern two-phase flows in microchannels: the Eötvös number ($Eo = \Delta\rho g D^2/\sigma$), and the Weber numbers of liquid and gas phases, namely, $We_l = \rho_l U_l^2 D/\sigma$ and $We_g = \rho_g U_g^2 D/\sigma$, where ρ_l and ρ_g are the densities of liquid and gas phases and $\Delta\rho = \rho_l - \rho_g$, U_l and U_g are the superficial velocities of liquid and gas phases, g is the acceleration of gravity, D is the inner diameter of a tube and σ is the surface tension. When all three parameters (Eo, We_l, and We_g) are less than unity, two-phase flow is more strongly affected by surface tension than by gravity and inertia force. At a fixed G, all three of these parameters (Eo, We_l, and We_g) and the Reynolds number (Re) decrease with decreasing tube diameter, and as a result, surface tension rather than buoyancy affects the two-phase flow, and the sheer stress at the gas–liquid interface decreases because the difference between the superficial gas and liquid velocities decreases.

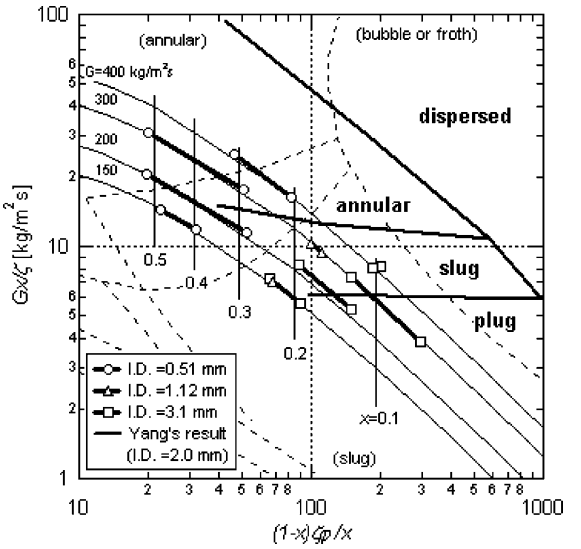

Fig. 4. Slug–annular flow transition and Yang's map on a modified Baker's flow pattern map for mass flux (G) from 150 to 400 kg/m^2 s.

Fig. 4 shows the slug–annular flow transition curves on a modified Baker's flow pattern map [20]. The results reported by Yang and Shieh for a 2.0-mm-ID tube [17] are also shown (bold lines and boldfaced letters on the map). The x at which slug–annular flow transition occurred increased with decreasing ID and G. These flow transition curves approximately coincide with those reported by Yang. Fig. 5 shows the flow patterns in the $G - x_{in}$ plane for the 3.1-mm-ID tube. The thick line in this figure expresses the transition point between slug flow and annular flow. With increasing G, the flow transition occurred at lower x_{in}. In the 3.1-mm-ID tube, oscillating flow (× and + in Fig. 5) occurred with different heated lengths of the tube, $L_{heat} = 1.62$ and 3.24 m, respectively. Once the oscillating flow occurred, h_{exp} decreased significantly at a wide range of x. For the 1.12-mm-ID tubes, oscillating flow occurred at low x_{in}, but for the 0.51-mm-ID tube, flow instability was not observed. Fig. 6 shows the neutral stability curves that dis- tinguish between unstable and stable regions in the 3.1-mm-ID tube for $x_{in} \approx 0$ and $4.00 \leqslant q \leqslant 19.81$ kW/m^2. The neutral stability points were obtained when q was decreased successively while G and the inlet vapor pressure were kept constant. Because oscillations in the

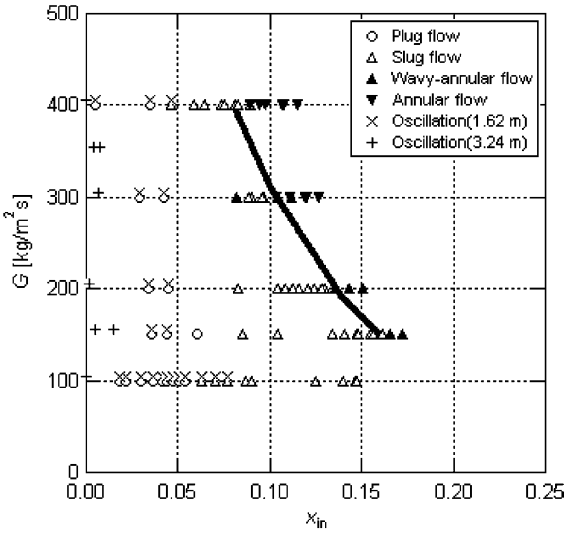

Fig. 5. Flow patterns and slug–annular flow transition in the $G - x_{in}$ plane for the 3.1-mm-ID tube. The symbols × and + represent the oscillating flow at $L_{heat} = 1.62$ and 3.24 m, respectively.

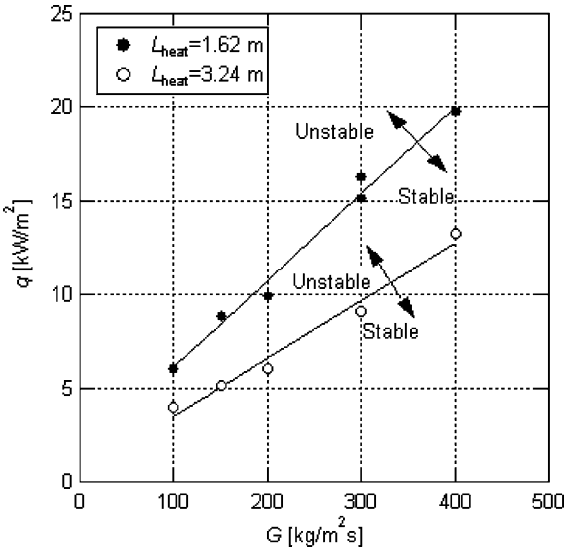

Fig. 6. Neutral stability curves for two different lengths of heated area, $L_{heat} = 1.62$ and 3.24 m, for the 3.1-mm-ID tube.

flow apparently coincided with oscillations in the outer surface temperature of the test tube, the neutral stability points can be obtained by monitoring the outer surface temperature. These experimental results suggest that the unstable region expanded with increasing q, decreasing G, or increasing L_{heat}. The time period of flow oscillations ranged from 0.8 to 4 s. Ding et al. [21] experimentally studied R-11 boiling flow in a 10.9-mm-ID horizontal channel, and reported three different types

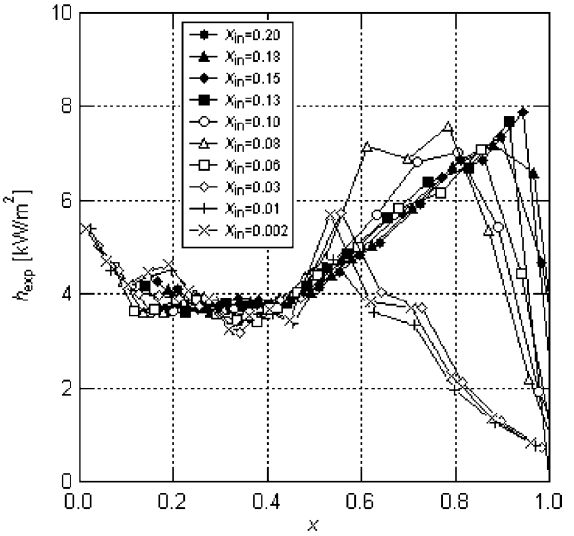

Fig. 7. Effect of inlet vapor quality (x_{in}) on boiling heat transfer coefficient (h_{exp}) for the 3.1-mm-ID tube for mass flux (G) of 300 kg/m^2 s and heat flux (q) of 13 kW/m^2.

of dynamic instabilities: (i) pressure drop oscillation; (ii) density wave oscillation and (iii) thermal oscillation. The time period of the density wave type oscillation was on the order of the transit time, that is, the time for density waves to travel between two ends of a channel [22–24]. In our experiments, because the transit time was about from 3 to 20 s, the oscillations observed here seem to be density wave oscillations.

Fig. 7 shows h_{exp} vs. x curves for the 3.1-mm-ID tube for various x_{in} at $G = 300$ kg/m^2 s and $q = 13$ kW/m^2. When $x_{in} \geqslant 0.13$, h_{exp} was almost the same. In contrast, when $x_{in} < 0.03$, flow instability occurred and h_{exp} was significantly reduced in the high x region. When $0.1 \leqslant x_{in} \leqslant 0.13$, the slug–annular flow transition seen in Fig. 5 occurred. This experimental result suggests that when the flow pattern at the entrance of a tube changes from annular flow to slug flow, h_{exp} decreases. For the 0.51-mm-ID tube, no such reduction in h_{exp} due to oscillating flow was observed.

3.3. Effect of evaporating temperature (T_{evap})

Fig. 8a and b show h_{exp} as a function of T_{evap} for the 3.1- and 0.51-mm-ID tubes, respectively. In the 3.1-mm-ID tube, T_{evap} did not significantly affect h_{exp}. In contrast, in the 0.51-mm-ID tube, h_{exp} increased with increasing evaporating temperature, and the effect of T_{evap} was significant in the high x region. In a high x region, the flow pattern is annular flow and the evaporation from a liquid film affects the flow boiling heat transfer. With increasing T_{evap}, the latent heat of vaporization decreases, the thickness of the liquid film decreases more rapidly, and h increases [25]. Pettersen

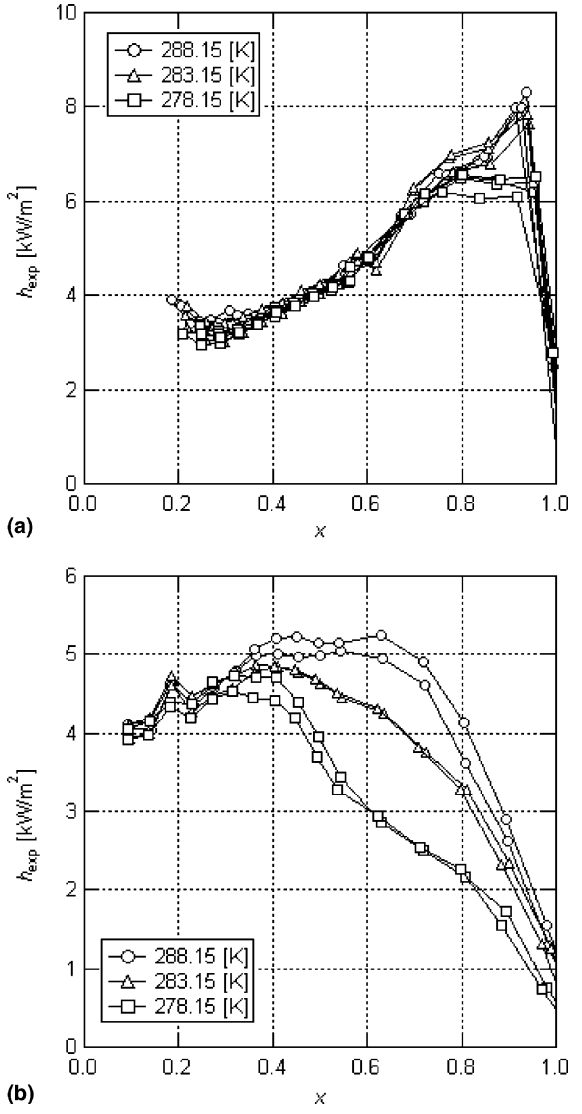

Fig. 8. Effect of evaporating temperature (T_{evap}) on boiling heat transfer coefficient (h_{exp}) for: (a) 3.1-mm-ID tube for mass flux (G) of 300 kg/m^2 s and heat flux (q) of 12 kW/m^2; (b) 0.51-mm-ID tube for $G = 300$ kg/m^2 s and $q = 14$ kW/m^2.

[26] investigated evaporation heat transfer for carbon dioxide flowing in a microchannel heat exchanger that had 25 channels that were 0.81-mm-ID, and showed that the h_{exp} increased with T_{evap} at $G = 280$ kg/m^2 s and $q = 10$ kW/m^2. In conclusion, the effect of T_{evap} on the boiling heat transfer increases with decreasing ID.

3.4. Boiling heat transfer coefficient (h_{exp}) vs Lockhart–Martinelli parameter (X)

The flow boiling heat transfer in a tube includes nucleate boiling heat transfer and forced convective evaporation. In forced convective evaporation, $h_{exp} \propto h_l(1/X)^n$, where h_l is the liquid phase heat transfer coefficient assuming no phase change occurs and X is the Lockhart–Martinelli parameter. Fig. 9 shows h_{exp} normalized by h_l, namely, h_{exp}/h_l, as a function of the reciprocal of the Lockhart–Martinelli parameter, namely, $1/X$. When the superficial liquid Re (Re_l) is smaller than 1000, flow in the liquid phase is laminar and $h_l = 4.36\lambda_l/D$. For the 0.51-mm-ID tube, the liquid flow was laminar over the entire range of G studied here (Fig. 9), whereas for the 1.12-mm-ID tube, the liquid flow was laminar only when $G < 150$ kg/m^2 s. In Fig. 9, the magnitude of forced convective evaporation can be expressed by the gradient n of a line fitted to the experimental data. The values for n suggest that as ID decreased, the liquid phase flow became laminar and the contribution of forced convective evaporation decreased.

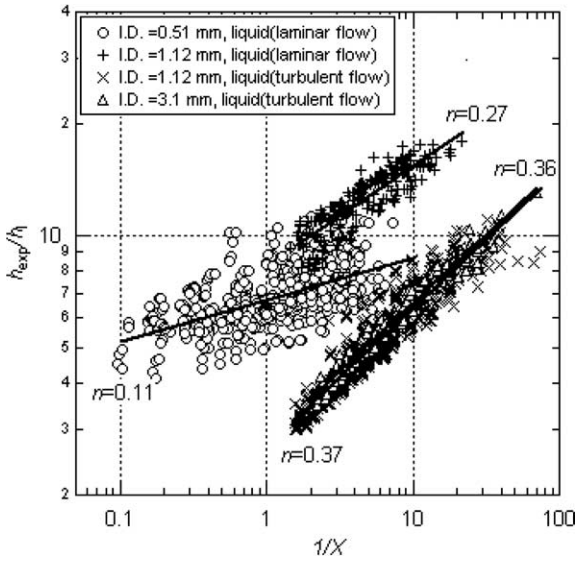

Fig. 9. Boiling heat transfer coefficient (h_{exp}) as a function of the Lockhart–Martinelli parameter (X). h_{exp} is normalized by the liquid phase heat transfer coefficient, h_l.

3.5. Pressure drop

The measured two-phase pressure drop (Δp) was compared with that predicted using the homogeneous model and that using the Lockhart–Martinelli's correlation. Because the ratio of acceleration pressure drop to the frictional pressure drop calculated using the homogeneous model was less than 10%, the acceleration pressure drop was negligible. In the homogeneous pressure drop model, the pressure drop is defined as

$$-\left(\frac{dp}{dz}\right) = \frac{2f_{TP}G^2}{\rho_h D} \quad (2)$$

where ρ_h is the density of homogeneous refrigerant and $1/\rho_h = x/\rho_g + (1-x)/\rho_l$, f_{TP} is a friction factor defined as $f_{TP} = 16/Re_h$ for laminar flow ($Re_h < 2400$) and as $f_{TP} = 0.079/Re_h^{0.25}$ for turbulent flow ($Re_h > 2400$), Re_h is the Re of homogeneous refrigerant and is defined as $Re_h = GD/\mu_h$, and μ_h is the viscosity of homogeneous refrigerant and is defined as $1/\mu_h = x/\mu_g + (1-x)/\mu_l$. In the Lockhart–Martinelli's correlation, the pressure drop is defined as

$$-\left(\frac{dp}{dz}\right) = -\left(\frac{dp}{dz}\right)_l \phi_l^2 = -\left(\frac{dp}{dz}\right)_g \phi_g^2 \quad (3)$$

where ϕ_l and ϕ_g are the two-phase multipliers in the liquid and gas phases, respectively, and are defined as $\phi_l^2 = 1 + 21/X + 1/X^2$ and $\phi_g^2 = 1 + 21X + X^2$ [27], where X is the Lockhart–Martinelli parameter, which is the square root of the ratio between the pressure drop assuming liquid flow alone and that assuming gas flow

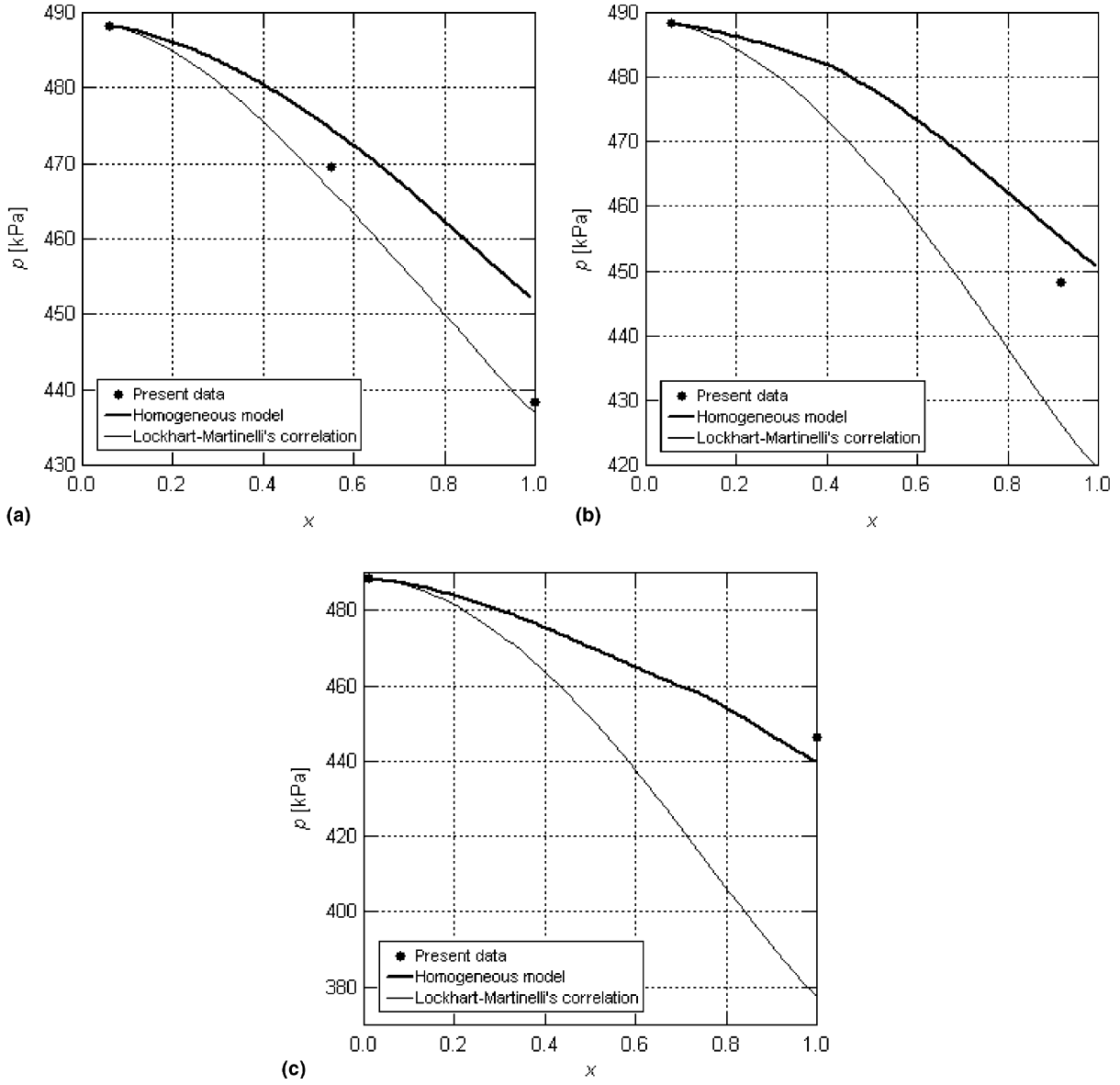

Fig. 10. Comparison between measured pressure drop and that predicted using a homogeneous pressure drop model and that using Lockhart–Martinelli's correlation for: (a) 3.1-mm-ID tube; (b) 1.12-mm-ID tube; (c) 0.51-mm-ID tube. For all three tubes, the mass flux (G) was 300 kg/m^2 s, and the heat flux (q) was 13 kW/m^2 for the 3.1- and 1.12-mm-ID tubes, and 15 kW/m^2 for the 0.51-mm-ID tube.

alone. Fig. 10a–c show the measured pressures and the pressures predicted using the homogeneous model and using the Lockhart–Martinelli's correlation as a function of x for the three tubes (3.1-, 1.12-, and 0.51-mm-ID). For the 3.1-mm-ID tube (Fig. 10a), the measured pressure agreed well with that predicted using the Lockhart–Maltinelli's correlation. In contrast, for the 0.51-mm-ID tube (Fig. 10c), the measured pressure agreed well with that predicted using the homogeneous model. For the 1.12-mm-ID tube (Fig. 10b), the measured pressure was between that predicted by these two different models. These experimental results suggest that with decreasing ID, the flow inside a tube approached homogeneous flow.

4. Conclusions

The effect of tube diameter on the boiling heat transfer of the refrigerant R-134a was investigated in horizontal small-diameter tubes of different diameter (0.51-, 1.12-, and 3.1-mm-ID). Local heat transfer coefficient (h_{exp}) and pressure drop (Δp) were measured for a range of heat flux (q) from 5 to 39 kW/m^2, mass flux (G) from 150 to 450 kg/m^2 s, evaporating temperature (T_{evap}) from 278.15 to 288.15 K, and inlet vapor quality (x_{in}) from 0 to 0.2. The following conclusions could be drawn from this study.

1. In the 3.1-mm-ID tube, h_{exp} increased with increasing mass flux or heat flux. In the 0.51-mm-ID tube, h_{exp} increased with increasing q, but was not significantly affected by G. In conclusion, the contribution of forced convective evaporation to the boiling heat transfer decreases with decreasing ID.
2. Dryout occurred in the lower x region with decreasing ID. In the 3.1-mm-ID tube, h_{exp} decreased when unstable flow was generated. In the 0.51-mm-ID tube, such unstable flow was not observed.
3. The x_{in} at the inlet of the evaporator affected the boiling heat transfer. When the flow pattern changed from continuous flow (annular flow) to intermittent flow (slug flow or plug flow), h_{exp} decreased at high x_{in}. In conclusion, the effect of T_{evap} on the boiling heat transfer increases with decreasing ID.
4. The frictional pressure drop was calculated based on the homogeneous model and also on the Lockhart–Martinelli correlation. With decreasing ID, the measured pressure drop was better predicted by the homogeneous model than by the Lockhart–Martinelli correlation. A plot of the dimensionless h_{exp} vs. Lockhart–Martinelli parameter suggests that as ID decreases, the flow in the liquid phase approaches laminar flow, and the effect of forced convective evaporation is suppressed.

Acknowledgements

This work was supported by a Grant-in-Aid for Scientific Research from the Japanese Ministry of Education, Culture, Sports, Science and Technology under Grant No. 13650212.

References

[1] S. Lin, P.A. Kew, K. Cornwell, Two-phase heat transfer to a refrigerant in a 1 mm diameter tube, Int. J. Refrig. 24 (2001) 51–56.
[2] S. Lin, P.A. Kew, K. Cornwell, Flow boiling of refrigerant R141b in small tubes, Trans. IChemE 79-A (2001) 417–424.
[3] G.M. Lazarek, S.H. Black, Evaporative heat transfer, pressure drop and critical heat flux in a small vertical tube with R-113, Int. J. Heat Mass Transfer 25 (1982) 945–960.
[4] Z.Y. Bao, D.F. Fletcher, B.S. Haynes, Flow boiling heat transfer of freon R11 and HCFC123 in narrow passages, Int. J. Heat Mass Transfer 43 (2000) 3347–3358.
[5] W. Yu, D.M. France, M.W. Wambsganss, J.R. Hull, Two-phase pressure drop, boiling heat transfer, and critical heat flux to water in a small-diameter horizontal tube, Int. J. Multiphase Flow 28 (2002) 927–941.
[6] T.N. Tran, M.W. Wambsganss, D.M. France, Small circular- and rectangular-channel boiling with two refrigerants, Int. J. Multiphase Flow 22 (1996) 485–498.
[7] M.W. Wambsganss, D.M. France, J.A. Jendrzejczyk, T.N. Tran, Boiling heat transfer in a horizontal small-diameter tube, ASME J. Heat Transfer 115 (1993) 963–972.
[8] W. Qu, I. Mudawar, Flow boiling heat transfer in two-phase micro-channel heat sinks. I. Experimental investigation and assessment of correlation methods, Int. J. Heat Mass Transfer 46 (2003) 2755–2771.
[9] B. Sumith, F. Kaminaga, K. Matsumura, Saturated flow boiling of water in a vertical small diameter tube, Exp. Therm. Fluid Sci. 27 (2003) 789–801.
[10] H.J. Lee, S.Y. Lee, Heat transfer correlation for boiling flows in small rectangular horizontal channels with low aspect ratios, Int. J. Multiphase Flow 27 (2001) 2043–2062.
[11] Y.Y. Yan, T.F. Lin, Evaporation heat transfer and pressure drop of refrigerant R-134a in a small pipe, Int. J. Heat Mass Transfer 41 (1998) 4183–4194.
[12] H.K. Oh, M. Katsuta, K. Shibata, Heat transfer characteristics of R-134a in a capillary tube heat exchanger, in: Proceedings of 11th IHTC, vol. 6, 1998, pp. 131–136.
[13] K. Kuwahara, S. Koyama, Y. Hashimoto, Characteristics of evaporation heat transfer and flow pattern of pure refrigerant HFC134a in a horizontal capillary tube, in: Proceeding of the 4th JSME-KSME Thermal Engineering Conference, 2000, pp. 385–390.
[14] P.A. Kew, K. Cornwell, Correlations for the prediction of boiling heat transfer in small-diameter channels, Appl. Therm. Eng. 17 (1997) 705–715.
[15] K.A. Triplett, S.M. Ghiaasiaan, S.I. Abdel-Khalik, D.L. Sadowski, Gas–liquid two-phase flow in microchannels. Part I: two-phase flow patterns, Int. J. Multiphase Flow 25 (1999) 377–394.

[16] A. Kawahara, P.M.-Y. Chung, M. Kawaji, Investigation of two-phase pattern, void fraction and pressure drop in a microchannel, Int. J. Multiphase Flow 28 (2002) 1411–1435.
[17] C.Y. Yang, C.C. Shieh, Flow pattern air–water and two-phase R-134a in small circular tubes, Int. J. Multiphase Flow 27 (2001) 1163–1177.
[18] C. Vlasie, H. Macchi, J. Guilpart, B. Agostini, Flow boiling in small diameter channels, Int. J. Refrig. 27 (2004) 191–201.
[19] S.M. Ghiaasiaan, S.I. Abdel-Khalik, Two-phase flow in microchannels, Adv. Heat Transfer 34 (2001) 145–254.
[20] D.S. Scott, Properties of cocurrent gas–liquid flow, Adv. Chem. Eng. 4 (1963) 199–277.
[21] Y. Ding, S. Kakaç, X.J. Chen, Dynamic instabilities of boiling two-phase flow in a single horizontal channel, Exp. Therm. Fluid Sci. 11 (1995) 327–342.
[22] V.P. Carey, Liquid–vapor Phase-change Phenomena, Hemisphere, Washington, DC, 1992, pp. 565–572.
[23] P. Saha, M. Ishii, N. Zuber, An experimental investigation of the thermally induced flow oscillations in two-phase systems, Trans. ASME 98 (1976) 616–622.
[24] H.C. Ünal, The period of density-wave oscillations in forced convection steam generator tubes, Int. J. Heat Mass Transfer 25 (1982) 419–422.
[25] A.M. Jacobi, J.R. Thome, Heat transfer model for evaporation of elongated bubble flows in microchannels, Trans. ASME 124 (2002) 1131–1136.
[26] J. Pettersen, Flow vaporization of CO_2 in microchannel tubes, Exp. Therm. Fluid Sci. 28 (2004) 111–121.
[27] D. Chisholm, A.D.K. Laird, Two-phase flow in rough tubes, Trans. ASME 80 (1958) 276–286.